Physicochemical investigations of native nails and synthetic models for a better understanding of surface adhesion of nail lacquers

Florian Laubé, Andy Poupon, Philippe Zinck, Christel Müller-Goymann, Stephan Reichl, Véronique Nardello-Rataj

▶ To cite this version:

Physicochemical investigations of native nails and synthetic models for a better understanding of surface adhesion of nail lacquers

Florian Laubé,[a] Andy Poupon,[a] Philippe Zinck,[a] Christel Müller-Goymann,[b] Stephan Reichl,[b] Véronique Nardello-Rataj*,[a]

[a] Univ. Lille, CNRS, Centrale Lille, ENSCL, Univ. Artois, UMR 8181 – UCCS – Unité de Catalyse et Chimie du Solide, F-59000 Lille, France. Corresponding author: veronique.rataj-nardello@univ-lille.fr.

[b] Institut für Pharmazeutische Technologie, Technische Universität Braunschweig, Braunschweig, Germany

Abstract

The human nail, like any biological material, is not readily available in large amounts and shows some variability from one individual to another. Replacing it by synthetic models is of great interest to perform reproducible and reliable tests in order to assess drug diffusion or nail lacquer adhesion for example. Keratin films, produced at the lab scale from natural hair, and the commercially available Vitro-nail® sheets have been proposed as models of human nails. In this study, we have investigated in detail these two materials. Surface aspect, composition, surface energy and water permeation were determined by SEM-EDS, ATR-FTIR, XPS, DVS and tensiometry and were compared to those of nails clippings. The development of a probe tack test using a rotational rheometer allowed us to measure the adhesion of three different nail lacquers on each substrate and the results were correlated with the surface state. It is shown that except roughness, keratin films exhibit similar composition, water sorption and surface energy as human nails. Vitro-nail® presents a more hydrophilic and permeable behavior than natural nail due to probable higher proportions of amide functions and absence of disulfide bridges. With the aim to improve nail lacquer residence, the importance of adsorption, electrostatic and mechanical adhesions as well as water sorption behavior is highlighted and allowed to show the importance of roughness, a low surface energy, a moderate hydrophobicity and an ability to form hydrogen and electrostatic bonds in order to optimize adhesion.

Keywords: Nail ; Nail lacquer ; Keratin film ; Vitro-nail ; Surface energy ; Adhesion
Words: 8231 including 1499 for the references
5 figures and 3 tables

1. Introduction

The human nail unit is a complex skin appendage ensuring several physiological functions. It has a protection and defense role due to its high hardness and flexibility, a grasping role allowing the manipulation of different objects, a sensation role to refine touch, as well as an esthetic role. All these properties result from its very particular structure. With an average thickness between 250 and 800 µm (Egawa et al., 2005; Gupchup and Zatz, 1999; Murdan, 2002; Saner et al., 2014; Täuber and Müller-Goymann, 2015), it consists of three parallel layers, *i.e.* dorsal, intermediate and ventral (Kobayashi et al., 1999; Murdan, 2002; Walters et al., 2012). Unlike the skin, the human nail contains high amounts of water which can vary from 2 to 35% depending on the relative humidity (Baden, 1970; Baden et al., 1973; Egawa et al., 2003; Khengar et al., 2007; Murdan, 2002; Walters et al., 2012; Wessel et al., 1999). In contrast, the lipid content is low, between 0.1 and 1%, mainly in the ventral and dorsal layers, which explains why nail is often described as a hydrophilic gel membrane with an additional lipophilic pathway (Gniadecka et al., 1998; Kobayashi et al., 1999; Mertin and Lippold, 1997; Walters et al., 1983). The relative permeability of nail plates allows the diffusion of drugs from pharmaceutical nail lacquers (e.g. varnishes, enamels, polishes) to treat diseases. Cosmetics lacquers are also concerned with permeability since in this case, the components should not diffuse into the body. The composition and the absorption ability of nails have been widely studied (Baden and Kvedar, 1993; Murdan, 2002; Walters et al., 2012). It has been reported that breaking physical interactions or chemical bonds between nail keratin fibers, such as disulfide, peptide, hydrogen or polar bonds, can potentially destabilize the nail barrier and improve the permeability of the nail plate (Gupchup and Zatz, 1999; Murdan, 2002; Wang, J.T; Sun, 1999). On the other hand, molecular weight, partition coefficient, hydrophilicity, pH and chemical nature of the vehicles have been identified as

potential factors allowing to improve the nail permeation (Gómez et al., 2018; Kobayashi et al., 2004; Murdan, 2002).

Murdan *et al.* reported the surface properties of nail plates such as surface energy (Murdan et al., 2012), pH (Murdan et al., 2011) and adhesion of nail lacquers (Murdan et al., 2015). However, unlike nail permeability studies, physicochemistry of nail surface and interactions with formulations of nail lacquers have been much less reported in the literature, in particular adhesion to nail plate. Adhesion can be described by four theories (Chaudhury et al., 1997; Kendall, 2001; Kinloch, 1987; Sharpe, 1998): *i)* the mechanical theory in which the substrate roughness allows an interlocking with the adhesive; *ii)* the adsorption theory which accounts for adhesion by attraction forces; *iii)* the electrostatic theory which considers that adhesion takes place by transfer of electrostatic charges and *iv)* the diffusion theory describing adhesion as the interpenetration of adhesives with substrate. If diffusion and adsorption theories with covalent bonds are unlikely and unwanted in case of nail lacquer, the other theories are conceivable, provided that there is a perfect wetting (Berg, 2010; Packham, 2011).

However, achieving such experimental physicochemical investigations on nails requires having representative and faithful models of human nail to carry out reproducible and reliable measurements. Indeed, natural nails are relatively diversified, : their properties change with gender, ethnicity or anatomical origin, fingernails and toenails present some differences. (Baden, 1970; De Berker and Forslind, 2004; Murdan et al., 2011). Moreover, nails are not easily available and expensive. Nail clipping can be used for permeation studies but they are not an ideal solution because of the limited nail bed and the available contact surface (Lusiana et al., 2011). To mimic nail surfaces, HDPE (high density polyethylene), glass or even steel are often used but they are not really representative of nails. In pharmacology, researchers have opted for animal materials such as porcine, sheep and bovine hooves (De Berker et al., 2007; Mertin and Lippold, 1997; Miron et al., 2014; Pittrof et al., 1992). The limitation of

similarities is the superior swelling of bovine hoof plates with water, until 45% (Lusiana et al., 2011), due to a more permeable keratin structure and probably to a lower concentration of half-cystine and disulfide linkages (Monti et al., 2005; Nogueiras-nieto et al., 2011; Täuber and Müller-Goymann, 2015). Moreover, animal tests can conduct to ethic issue, particularly in cosmetic industry. Due to these constraints, artificial nail models have been proposed such as keratin films developed by Lusiana *et al.* based on keratin extracted from hairs (Lusiana et al., 2013, 2011; Täuber and Müller-Goymann, 2015). Indeed, hair and nail are two keratinous materials with similar composition (Baden and Kvedar, 1993; Gniadecka et al., 1998; Gupchup and Zatz, 1999; Williams et al., 1994). In the same way, IMS Ltd Company has developed a synthetic nail plate model, named Vitro-nail®. Both these models are relatively new and have not been extensively studied yet.

Thus, we report herein a comparative characterization of nail clippings (NC) with keratin films (KF) and Vitro-nail® (VN) in terms of composition, surface state and water absorption. Adhesion of three nail lacquers on the different substrates was investigated using a rotational rheometer. The results were discussed according to the formulation of the nail lacquers and the surface of the substrate models in comparison to that of the nail.

2.   Materials and methods

2.1.   Materials

2.1.1. *Substrates*

Nail clippings (NC), relevant to free edges of nail units, were from fingers of five female volunteers of different ages and ethnic origins. They were ≈ 0.5x1 cm, washed in technical ethanol then dried at room temperature (23 ± 2 °C) and humidity (50 ± 5%). Keratin films (KF) were prepared from keratin extracted from natural blond hairs according to the

procedure described by Lusiana *et al.* (Lusiana et al., 2011; Täuber and Müller-Goymann, 2015). Each sample had a diameter of 1.5 cm and a thickness of ≈ 75 µm. Vitro-nail® (VN) sheets (surface 20 cm², thickness of 500 µm) were purchased from IMS, Milford, CT. Their composition has not been reported but according to IMS, it is expected to mimic the wetting properties, thickness and flexibility of human fingernails. Nail clippings, keratin films and Vitro-nails® were placed under similar hydration and temperature conditions (*i.e.* 25 °C and air moisture at 45% for 24h) before any analysis.

2.1.2. *Nail lacquers*

Nail lacquers contained a film forming polymer (10 to 20%), a resin (7 to 15%) to improve film adhesion, shine or hardness, a plasticizer, a large amount of solvents (65 to 75%) and additives such as pigments (1 to 10%) typically used in cosmetic nail lacquers. Formulations were obtained mixing a base containing the majority of film forming polymer, resin, plasticizer, solvents, rheological agent, with a color paste containing milled pigments in film forming agent and solvents. Three nails lacquers were used for adhesion tests: 1) a lacquer with a good adhesion, noted "NL-GA", based on nitrocellulose as a film forming agent and an epoxy tosylamide resin; 2) a lacquer with a poor adhesion, noted "NL-PA", consisting of acetobutyrate cellulose as a film forming agent and a polyester resin; and 3) a lacquer noted "NL-GA+colored", of same composition as the first one but with colored mineral pigments. The three formulations had the same plasticizer, the same ester solvents (dry extract content = 29 %) and similar proportions of the components. Their viscosity and rheological behavior were also similar (viscosity μ = 1080 ± 60cP measured with a Brookfield viscometer at 60 rotations per minute).

2.2. **Surface analysis**

2.2.1. Surface state

Scanning Electron Microscopy (SEM) with X-Ray mapping (SEM-EDS)

The specimens for SEM characterizations were cut in fragments of 0.5 cm² before carbon metallization. SEM images were obtained at 5.0 kV for nail clippings and keratins films and at 10.0 kV for Vitro-nails® under high vacuum conditions on a Jeol JCM6000 PLUS microscope. The samples were also characterized by EDS to detect the different elements present and to realize mapping.

Profilometer

The arithmetic mean roughness or mean deviation (Ra) of the different surfaces was determined on an Alfa Step IQ surface profilometer (KLA-Tencor). The cantilever traveled at 20 μm/s on 1000 μm long sections. Results are average of at least four measurements on different areas of the samples.

2.2.2. Chemical composition of substrates surfaces

Fourier Transform InfraRed (ATR-FTIR)

ATR-FTIR measurements were performed on a Brucker Vertex70 Fourier Transform Infrared Spectrometer coupled with a universal diamond ATR and an RT-DLa TGS detector was used to scan the different samples. The source was Mid-infrared spectral region, the separator was KBr and the reflectance crystal was 6 mm in diameter. Each spectrum was the average of thirty-two scans from 4.500 to 350 cm^{-1} with a resolution of 4 cm^{-1} and a scanning frequency of 10 kHz. For each material, two to four samples were used and for each material, the analysis was realized two to three times at different locations on the top and on the bottom.

X-Ray Photoelectron spectrometry (XPS)

Chemical composition characterizations of the different surfaces were performed by XPS. Analyses were carried out with a Kratos Axis Ultra spectrometer using a monochromatic Al

Kα source (15 mA, 15 kV). Instrument base pressure was 8×10^{-10} Torr. C 1s, O 1s, N 1s, Na 1s, S 2s, S 2p, Si 2p, and Ca 2p high-resolution spectra were collected using a 40 eV pass energy. The Kratos charge neutralizer system was used for all analyses. Spectra were charge corrected to give the carbon C 1s spectral component C-(C,H) a binding energy of 285 eV.

2.3. Surface energy measurements

In order to determine the surface energy of the different materials, contact angles of 8 solvents were measured with a Krüss DSA100 tensiometer supported by Advance software. The solvents were chosen to reach a large range of polarity and to calculate the surface energy very accurately (see Supporting Information). According to Young's equation, there is a relationship between contact angle θ, the surface tension of the liquid γ_L, the interfacial tension between liquid and solid γ_{SL} and the surface free energy γ_S. In order to calculate γ_S from the contact angle, the second unknown variable γ_{SL} has to be determined. Owens-Wendt (Eq. 1) (Owens and Wendt, 1969) and Wu (ASTM D 2578-67) (Eq. 2) (Wu, 1982) developed equations which allow to calculate the surface energy, *i.e.* dispersive (γ_S^D) and polar (γ_S^P) components.

$$\textit{Owens-Wendt} \qquad \gamma_{SL} = \gamma_S + \gamma_L - 2\left[\sqrt{\gamma_S^D \gamma_L^D} + \sqrt{\gamma_S^P \gamma_L^P}\right] \qquad (1)$$

$$\textit{Wu} \qquad \gamma_{SL} = \gamma_S + \gamma_L - 4\left[\frac{\gamma_S^D \gamma_L^D}{(\gamma_S^D + \gamma_L^D)} + \frac{\gamma_S^P \gamma_L^P}{(\gamma_S^P + \gamma_L^P)}\right] \qquad (2)$$

The first method is commonly used in industry, the second one is considered as more mathematically rigorous than O-W (due to mathematic determination: Wu employed a harmonic average whereas O-W used a geometric average) and mostly used for the calculation of surface energy for polymers with low surface free energy (up to 40 mN.m^{-1}).

2.4. Water permeation determination

Dynamic Vapour Sorption (DVS)

Water absorption ability of materials was accurately determined with a dynamic vapor sorption apparatus TA Instruments DVS Q5000. Fragments of 3 to 6 mg of materials were directly weighed onto sample pans previously set. Each pan was placed in a chamber with constant flow of dry nitrogen with a flow of nitrogen and water vapor. Then, two methods with accurate conditions of temperature (T) and relative humidity (RH) were imposed: *i)* T fixed at 30 °C, RH varying from 5 to 95%; *ii)* RH fixed at 45%, T varying from 5 to 55 °C (see details in Supporting Information). Sample mass was monitored with a microbalance. To overcome variations due to sample thickness, the different materials were also milled in powder at very low temperatures using a Retsch Cryomill with N_2 liquid autofilling. Fragments of each material were placed in grinding jar (25 mL capacity) with a grinding ball (diameter of 15mm), both composed of zirconium oxide. After a precooling step of 5 min, the grinding jar was shaken at 30 Hz for 5 min. Then, powder grain size was estimated with a Keyence VHX optical microscope supported by a Z20 lens.

2.5.   Nail lacquer adhesion

Work of adhesion (Wa) – thermodynamic adhesion

The work of adhesion (Wa) of nail lacquers to each material surface was calculated using the Young-Dupré equation. For that, the surface tension of the lacquer γ_L was measured at T = 25± 1 °C using a Krüss DSA10 tensiometer and a Wilhelmy plate as a probe immersed into the lacquer at a rate of 10 mm·min^{-1} and on 2 mm depth. Before each series of measurements, calibration with pure water was carried out (72 mN/m at 25 °C). Then, Wa was determined according to the equation $Wa = 2\sqrt{\gamma_S \gamma_L}$ in which it is considered that dispersion forces as dominating (Berg, 2010).

Probe tack test: removal resistance – mechanical adhesion

To characterize mechanical adhesion, a probe tack test was developed using a Malvern Kinexus Ultra+ rheometer with disposable plates. The superior plate (SP) was a disk of 25 mm diameter clamped with two screws to rotatable rod, whereas the inferior plate (IP) was a disk measuring of 63 mm diameter, clamped to inferior platform with three screws. First, a substrate piece (nail, keratin film or Vitro-nail) measuring between 0.1 and 0.6 cm² was glued to the IP using a two-component epoxy glue (SÄDER® RAPIDE). After one night, the three nail lacquers were uniformly applied on substrate surface with a standard nail lacquer brush (Two strokes). After a second night of drying and rheometer calibration, SP and IP, with substrate and lacquer, were clamped on rheometer. Fresh glue was deposited on the nail lacquer due to the extremity surface of a standard 1/16'' allen key. The SP was lowered at the IP level applying a force of 0.5 N to glue the two parts. After 10 min, the assembly (IP-glue-material-lacquer-glue-SP, see **Fig. S6**) was softly unclamped of rheometer and let under pressure during one night. The next day, the assembly was softly clamped back to the rheometer and the probe tack test program was started. The rheometer applied an upward vertical force to ascend at a speed of 0.1 mm.min^{-1} until breaking. The maximum strength was retained. A visual observation allowed to identify the kind of failure: cohesive or adhesive. A Keyence VHX optical microscope supported by a Z20 lens was used to measure nail lacquer surfaces stripped in case of adhesive failure. Then, the maximum stress was calculated dividing strength by stripped surface.

3.   Results and Discussion

3.1.   Surface analysis of nail plates and models

Surface aspects and profilometry

The nail surface, corresponding to the dorsal part, was first examined by SEM (**Fig. 1a**). As described in the literature (Murdan, 2002), the surface is an overlay of scales of ≈ 50 µm.

Many cracks, scratches and a few impurities can be observed. Nevertheless, the surface is globally homogeneous with a slight relief and anchor points allowing a mechanical adhesion.
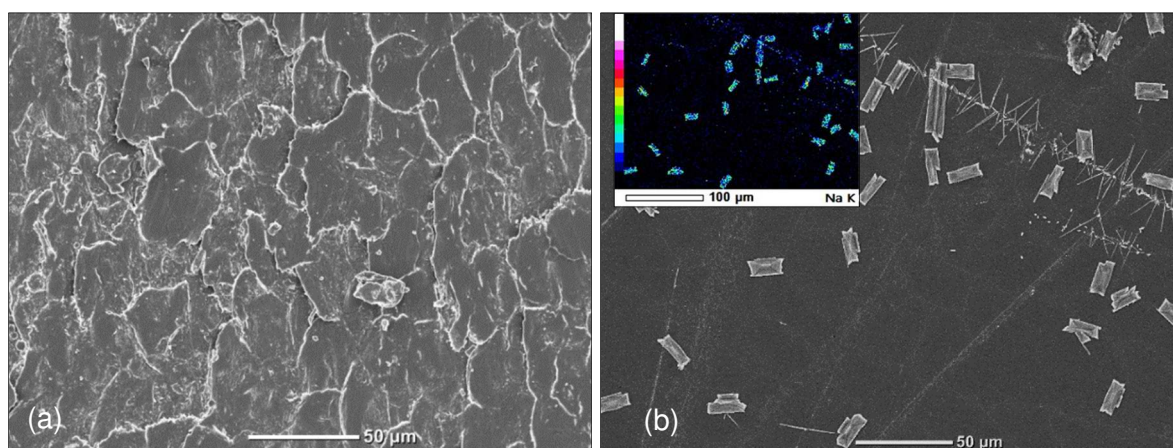

Fig. 1. Scanning electron micrograph of nail clipping surface (high vacuum, 5.0 kV, × 400 magnification) (a); and Scanning electron micrograph of Vitro-nail® top surface (high vacuum, 10.0 kV, × 400 magnification) and SEM-Energy Dispersive X-ray Spectroscopy of sodium on Vitro-nail® top surface (b).

On the contrary, when hydrated, keratin films possess an extremely smooth surface on both sides. The lack of relief does not allow obtaining micrograph with sufficient resolution. The smooth surface arises from the manufacturing process, that are films originating from mixture poured into polytetrafluoroethylene on a siliconized polyethylene terephthalate. However, films completely dried can present macroscopic wrinkles that are inconvenient for the targeted application. At first sight, Vitro-nails® exhibit a similar surface since there are no reliefs on both sides, in agreement with information from the supplier. Nonetheless, one side shows some scratches and little crystals (10-20 µm of length) (**Fig. 1b**), which correspond to Na_2SO_3 or Na_2SO_4 crystals according to X-Ray mapping (SEM-EDS) detailed above (**Fig. 1b**).

To confirm these first observations and quantify the nail plate relief, roughness was measured more specifically witha profilometer. Measurements were performed on four sources of nail clippings in two directions: the natural nail growth direction and the transversal direction. Similarly, two different batches of KF and VN were used and analysed

in two perpendicular directions on both sides. The roughness parameter *Ra*, which is the arithmetical mean deviation of the assessed profile and which is more widely used for roughness quantification, was retained (see details in Table S1). Therefore, Ra = 308 ± 52 nm for NC, 15 ± 6 nm for KF and 18 ± 5 nm for VN. Each result is an average of 5 measurements: undergrowth and transversal axis from four origins for NC, on top and bottom of two different samples for KF, and on top and bottom of one sheet for VN. For the three substrates, results are in agreement with the SEM observations. Regarding native nail, there is a slight roughness with an average depth around 300 nm, without significant differences depending on the sample sources or the scanning directions. This roughness could be responsible for a part of adhesion by interlocking. On the contrary, roughness is very low for KF and VN, and can be considered as zero, the intrinsic uncertainty of profilometer being about 9 nm. Hence, the potential adhesion of a nail lacquer on these two substrates could not be due to mechanical adhesion. This highlights a first significant difference of these models with natural nail plate which is about twenty times rougher.

Composition of the different surfaces

The composition of the three substrates was determined with a SEM-Energy Dispersive X-ray Spectroscopy (SEM-EDS). Carbon, oxygen, sulfur and nitrogen were mainly identified for nail clippings, due to the presence of amino acids that naturally composed the nail keratin (Baden and Kvedar, 1993; Gupchup and Zatz, 1999). Minerals such as calcium, magnesium, aluminum, silicon and sodium were also detected in lower proportions, in agreement with the literature (De Berker et al., 2007; Gupchup and Zatz, 1999; Murdan, 2002). Repartition of all these elements is perfectly homogeneous and was confirmed by means of mappings similar to the one in **Fig. S1b**. Regarding keratin films, except sodium, the same elements and same homogeneity were observed on both sides of different samples, but the sulfur intensity was

stronger. This can be explained by the higher amount of sulfur in keratin hair due to a greater proportion of cysteine, favoring disulfide bridges (Baden et al., 1973; Gupchup and Zatz, 1999). These bridges reinforce the keratin fibers cohesion providing a harder keratin, sometimes called hair-type keratin in contrast with the softer skin-type keratin (Lynch et al., 1986). Besides, Lynch *et al.* determined that hair-type keratin forms 80% of the nail plate keratin but it is mainly present in the intermediate layer of nail whereas skin-type keratin, poorer in sulfur, is found in the dorsal and ventral layers. This can explain why nail samples contain less sulfur than keratin films since SEM-EDS analyzes the dorsal layer. The main elements detected in Vitro-nails® were carbon, oxygen, nitrogen and sodium, with traces of sulfur, phosphor and chlorine. **Fig. 1b** shows that a few elements are distributing with some heterogeneity: sodium and sulfur were mostly present and oxygen was more concentrated in little solids corresponding probably to crystals of Na_2SO_3 or Na_2SO_4. Indeed, these components, only present on the top face, could have been used as reducing agent during the manufacturing process. The rest of the matrix is homogeneous and contains carbon, oxygen and nitrogen suggesting that Vitro-nails® may be composed of another keratin or protein. The absence of significant sulfur amount in the matrix is the main difference to KF and nail plate.

ATR-FTIR analyses were then performed on the three substrates (**Figures 2 and S2**). The FTIR spectra of nail clippings present the different vibrational modes of the amide bonds, from different individual amino acids of keratin, lipids and fatty acids, bonded water and some trace elements. This is in agreement with the literature (Gniadecka et al., 1998; Lehtinen, 2013; Sowa et al., 1995; Wang et al., 2016) (details are given in Supporting Information).
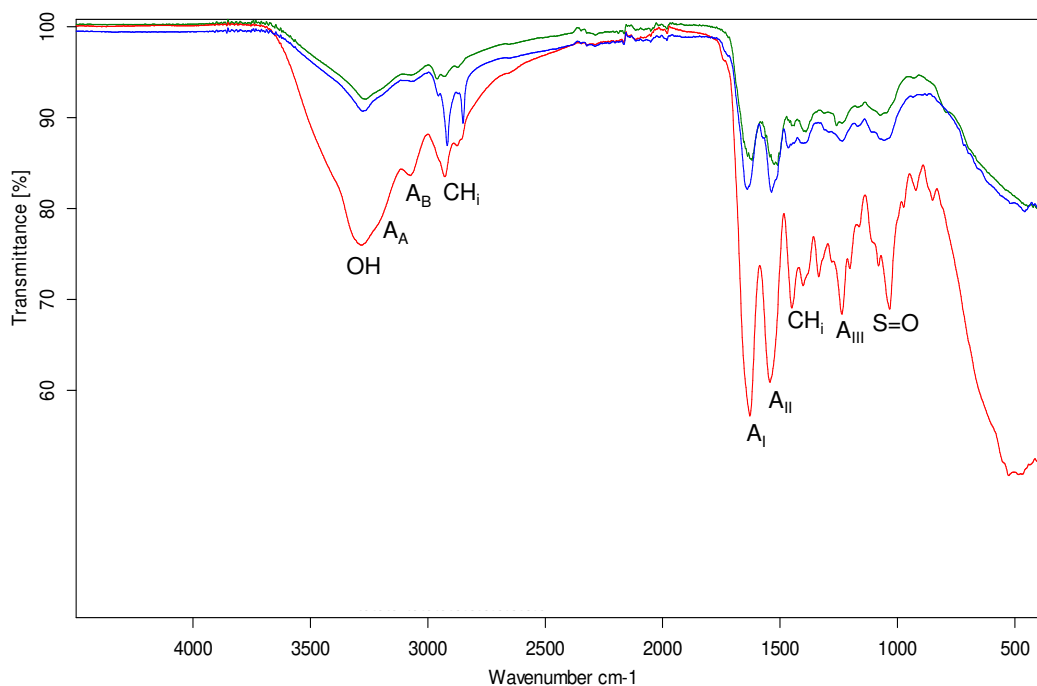
Fig. 2. FTIR-ATR spectra of natural nail clipping (blue) in comparison with keratin film (green) and Vitro-nail® fragment (red). Notations: A_A, A_B, A_I, A_{II}, A_{III} respectively correspond to amide A, B, I, II and III (vibrational modes). CH_i corresponds to CH_2 and CH_3, OH represents bonded water and S=O corresponds to sulfoxide functions.

As expected, KF and nail spectra are very similar. The only significant difference is the lower intensity of the peaks between 2900 to 3075 cm^{-1} indicating a smaller amount of alkyl functions and of lipids and fatty acids in KF which can be removed during the keratin extraction step. Vitro-nail® exhibits two additional peaks: one at 1335 cm^{-1} which could also correspond to alkyl groups and a more intense one at 1035 cm^{-1} which could represent sulfoxide functions (Lehtinen, 2013), in agreement with the presence of crystals. Nevertheless, the amides peak shapes and intensities vary notably for Vitro-nail® suggesting that they contain a very different keratin or more probably, another protein. Similarly, VN presents also more intense peaks at 3450-3500 cm^{-1}, whose intensities depend on the amount of bonded water.

Finally, chemical composition was also investigated with XPS. Nail keratin composition has already been determined by RAMAN spectroscopy (Baden et al., 1973; Gupchup and Zatz, 1999; Saeedi et al., 2018). Nevertheless, XPS explores materials on the extreme surface

13

(≈ 10 nm) and allows the accurate detection of the elements and their chemical environment.
Table 1 reports the relative proportions of the elements detected by XPS for the three substrates, each value being an average of several measurements performed on two different samples.

Table 1
Relative proportions of elements detected by XPS for nail clippings (NC), keratin films (KF) and Vitro-nail®(VN) fragments. Each sample was washed with isopropyl alcohol before any analysis.

Elements (relative %)	NC	KF	VN
C	72.6±1.8	61.3±0.9	66.6±3.1
O	19.6±2.3	24.0±2.4	18.2±1.4
N	6.2±0.9	5.4±1.0	14.6±1.8
S	0.4±0.1	0.5±0.1	0.2±0.0
Si	0.6±0.1	8.9±1.0	*nd*
Ca	0.5±0.1	*nd*	*nd*
Na	*nd*	*nd*	0.4±0.1
Ratios			
O/C	0.27	0.33	0.27
N/C	0.09	0.14	0.22
S/C	0.01	0.01	0.00
Si/C	0.01	0.12	*nd*

nd: not detected.

XPS confirms the results obtained by SEM-EDS. When comparing the relative proportions of the main elements, *i.e.* carbon, oxygen and nitrogen, we notice some significant discrepancies between the three substrates. Indeed, NC contains more carbon over KF and VN while KF contains more oxygen and VN more nitrogen. Besides, the main difference is due to the unexpected high percentage of silicon in KF which can be accounted for by the film preparation method which uses siliconized polyethylene terephthalate (PET) foil as a molding base (Lusiana et al., 2011). Vitro-nail® and nail clipping compositions are quite close with the exception of a higher amount of nitrogen element, probably due to more amide functions. The fit of elements spectra obtained with Gaussian (see **Fig. S3**) allows the determination of the binding energies of each element and the chemical environment as summarized in **Table 2**.

Table 2
Potential chemical environments for each binding energy of elements detected by XPS for nail clippings, keratin films and Vitro-nail® fragments.

Elements	Binding energy (eV)	Chemical environment proportion (% per element)			
		Potential chemical environment	NC	KF	VN
C1s	285.0	**C-C/C-H**	65	59	42
	286.4	**C-O/C-N**	23	25	34
	288.4	**O-C=O/ N-C=O**	12	15	25
O1s	531.7	**C=O**	60	100	76
	532.9	**C-O-H**	40	0	24
N1s	400.2	**C-N-H**	100	100	100
S2p$^{3/2}$/S2p$^{1/2}$	163.8/165.0	**C-S-S-C/ C-S-H**	49	81	21
a	168.2/169.4	**SO$_3^{2-}$**	51	19	80

[a]$2p^{3/2}$-$2p^{1/2}$ doublet separation = 1.18eV.

XPS spectra of carbon and oxygen reveals the expected C-N, C-O, O=C-O, O=C-N (carbon environment) and C=O, C-OH (oxygen environment) functions mainly due to amino acids (in particular glutamic acid, serine, cystine, threonine) and peptide linkages(Baden et al., 1973; Gupchup and Zatz, 1999). Only one binding energy was detected on nitrogen spectra; it corresponds to a C-N-H environment and confirms the presence of amide functions at nail plate surface, preferentially primary and secondary amides, likely to form hydrogen bonds with the formulations. Regarding binding energies of sulfur, the present of S-H bond could also play a role in adsorption. Electrostatic (or coulombic) interactions are also plausible because nail pH is ≈ 5 (Murdan et al., 2011) *versus* ≈ 7 for nail lacquers, allowing the presence of both negatively charged carboxylic acid groups COO$^-$ and positively charged amino groups NH$_3^+$ (pK$_{a(COOH/COO^-)}$ = 1.7 to 3.5 and pK$_{a(NH_3^+/NH_2)}$ = 7.5 to 10.8 for free or linked amino acids (Doig and Baldwin, 1995; Herries, 1985)).

As expected, keratin films exhibit a surface chemical environment very close to the one of the nail: keratin from hair and keratin from nail have both great proportions of glutamic acid (12.2% for hair *vs* 13.6% for nail), serine (12.2 *vs* 11.3%) and half-cystine (15.9 *vs* 10.6%) (Baden et al., 1973; Gupchup and Zatz, 1999). There are only two significant differences regarding O1s and S2p: the absence of alcohol function and the greater proportion of thiol and/or disulfide, certainly due to differences in cystine amount. Vitro-nail® contains more amide and carboxylic functions than nail plate. The most important discrepancy is the thiol/disulfide proportion since the presence of sulfur, very weak (see **Table 1**) is largely due to crystals of Na_2SO_3 and not to cystine. This difference could be useful to determine the impact of sulfur bonds in adsorption adhesion (see below).

3.2. Surface energy determination

In order to determine surface energy of nail clipping, keratin film and Vitro-nail®, contact angles of 8 solvents were measured (see **Table S2**). KF and VN were analyzed on both sides but no difference was observed. It is important to note that the three materials are porous and absorb some solvents, especially water, as detailed in Section 3.3. This can lead to variable contact angles values as confirmed by the very different values found in the literature (Murdan et al., 2012). Hence, it is very important to measure the contact angle at a same and very short time (5 s here). At first sight and as indicating by the increasing contact angles of the eight solvents from VN to NC, it seems that VN is more wettable than KF, which is more wettable that nail clipping. In addition, the different roughness of NC and KF does not seem to have a strong impact, the differences being slight, in particular for water (89° for NC vs 85° for KF). On the contrary, the gap is more important with VN (76°) and cannot be only due to roughness but probably to a bigger polarity.

Surface energies of NC, KF and VN were then calculated with the models of Owens-Wendt (OW; extension of Fowkes model) and Wu. These models allow the determination of

the polar γ_S^P and dispersive γ_S^D components of the substrates. **Fig. 3** presents the values obtained. The surface energy of NC was found to be 28 ± 2 mJ/m² according the OW model and 32 ± 2 mJ/m² according to Wu. These values are in good agreement with that of Murdan *et al.* (*i.e.* 34 ± 4 mJ/m²) which was determined using the Van Oss model (Murdan et al., 2012).
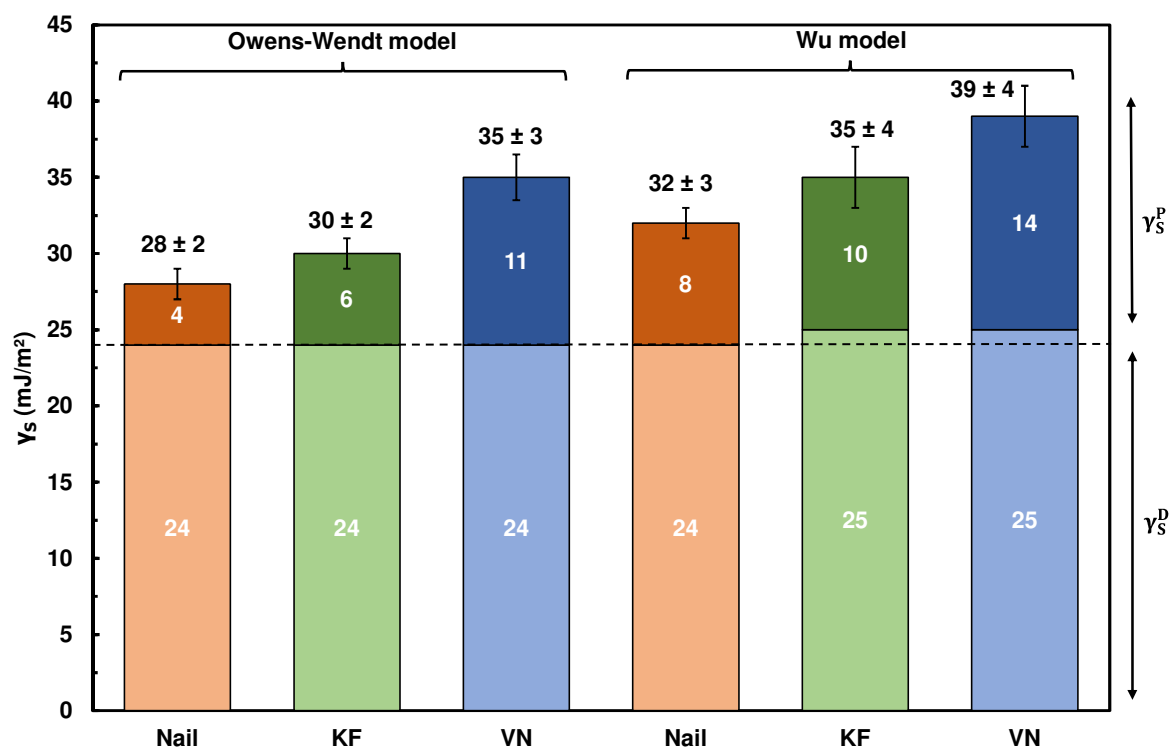

Fig. 3. Surface energy γ_S as well as polar γ_S^P (dark colors) and dispersive γ_S^D (clear colors) components of nail, keratin film and Vitro-nail® surfaces determined by the sessile drop method and calculated with the Owens-Wendt and Wu models.

Surface energy of KF as well as the polar and dispersive components are close to that of nail. Vitro-nail® has a slightly higher surface energy mainly due to a higher polar component which could have a direct impact on the thermodynamic adhesion and the nail lacquer spreading. The components used for the preparation of the Vitro-nail®, probably amino acids and/or proteins, should be responsible for this higher polarity. It is noteworthy that Rizi *et al.* have recently reported the surface energy of Vitro-Nail® (Rizi et al., 2018). Though slightly

higher, their value (50 mJ/m^2) is consistent with ours. The difference is explained by the use of another model.

3.3. Water permeation study

Water contact angle

The three materials exhibit significant water permeation. The kinetic evolution of the water contact angle on the three materials is shown in **Fig. S5** (Supporting Information). NC and KF have a similar behavior with a slow decrease from 85-90° to 20° in 40 min, mainly due to absorption and to a much lesser extent to water evaporation once the material is saturated [42]. VN absorbs water faster from 75 to 42° in 13 min, then there is a second slope, certainly due to evaporation, from 42 to 20° in 35 min. The VN ability to absorb water is in agreement with the peaks of hydrogen-bonded water observed by FTIR.

Dynamic vapor sorption

To quantify and compare the water absorption, evolution of the moisture content of nail, keratin film and Vitro-nail® was monitored by Dynamic Vapour Sorption (DVS). As the materials exhibit different thicknesses (200 to 800 µm for NC, 65 to 80 µm for KF, and ≈ 535 µm for VN), the measurements were carried out on substrate powders. The grain sizes of powders obtained were determined by means of optical microscope and were between 20 and 50 µm. Firstly, an isotherm program at 30 °C was used to study the room humidity dependence of the materials. The program consisted of one drying step followed by one-step during which the humidity was increased gradually from 5 to 95% of relative humidity. The profiles of samples weight evolution are given in Supporting Information (**Fig. S6**) and results are summarized in **Table 3**. It is noteworthy that samples did not contain same amounts of water initially, showing the importance of the drying step. The values at t_0 are lower than expected (from 7 to 20%) but are consistent since Stern *et al*. showed that nails were losing water between the time of clipping and analyses (Stern et al., 2007). The samples were placed

in humidity chamber a few days before any other analysis. Concerning the absorption step, NC and KF powders behave similarly in term of speed, time and water content. This finding strengthens already observed similarities in terms of composition and surface energy and suggests that nail properties are logically and mainly due to keratin properties.

Table 3
DVS analysis with program of A) isotherm (T = 30 °C), relative humidity ramp (H = 5-90%) and B) fixed relative humidity (H = 45%), temperature ramp (T = 5 to 55 °C), for nail, keratin film and Vitro-nail® under fragment and powder forms.

A) Fixed temperature T = 30 °C, relative humidity ramp (RH = 5-90%)					
	Drying step		**Absorption step**		
Sample	Water content at t_0 (%)	Drying speed (%/h)	Absorption speed (%/h)	Water content at t_f (%)	Final time (h)
NC[a]	6.5	0.2	0.2	18.6	146
KF	5.7	0.7	0.2	18.1	81
VN	3.5	0.1	0.3	40.5	160
NC powder[a]	7.3	1.3	0.3	16.9	55
KF powder	6.5	0.8	0.3	17.7	69
VN powder	12.0	2.0	1.5	44.5	35

B) Fixed relative humidity RH = 45%, temperature ramp (T=5-55 °C)		
	Drying step	**Absorption step**
	Drying speed (%/h)	Water Content maximum (%)	Final time (h)
NC[a]	1.6	2.6	35
KF	3.1	3.6	20
VN	0.9	0.6	42
NC powder[a]	10.9	7.9	22
KF powder	6.7	6.5	24
VN powder	-	2.2	7

[a] average of measurements performed on 4 different sources.

Vitro-nail® has a much higher capacity to absorb water. Indeed, though the absorption speed is of the same order of magnitude, the final water content reaches 40.5 wt%. This value confirms that VN is probably more hydrophilic probably due to the presence of more amide functions which favor hydrogen bonds, and due to the low amount of disulfides bridges. As

shown on **Fig.5**, based on DVS isotherm analyses, the moisture content at equilibrium in the samples can be determined for each relative humidity.
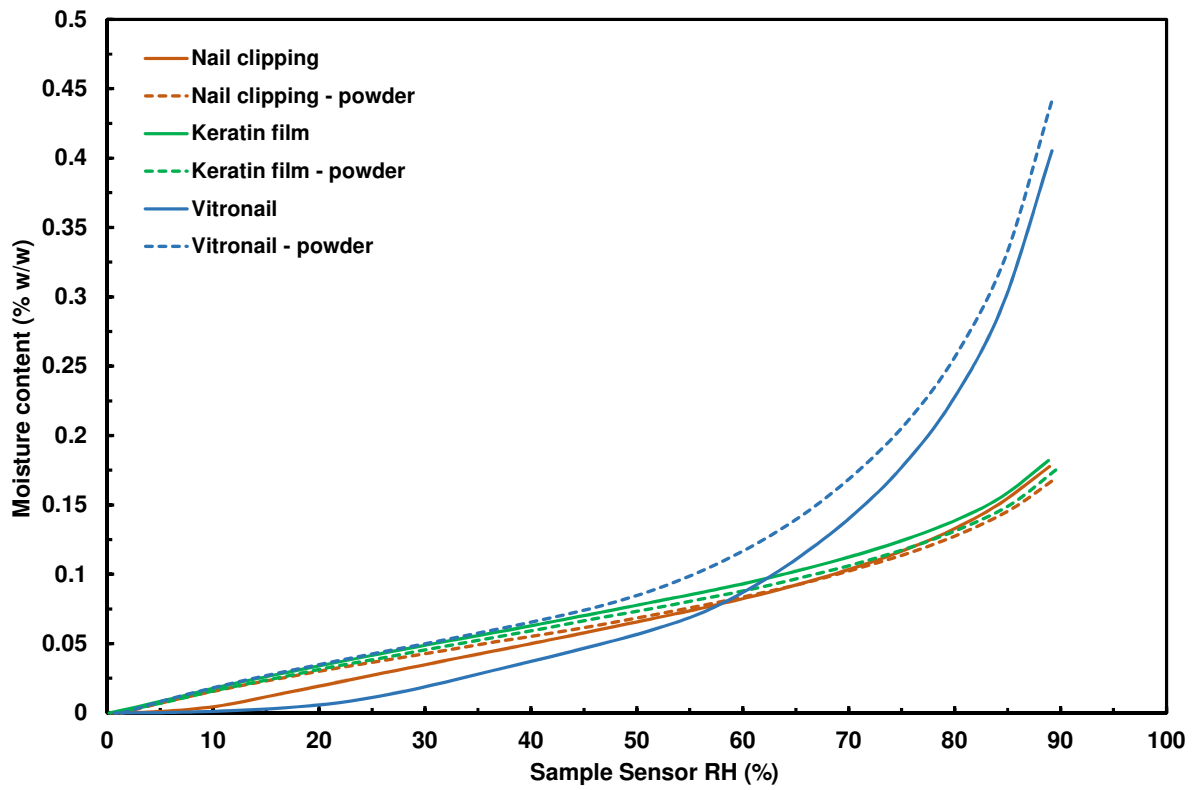

Fig. 4. Isotherm water sorption (T = 30 °C) for nail, keratin film and Vitro-nail® under fragment and powder form (moisture content = mg H_2O/100 mg sample; RH = Relative Humidity)

We observe that KF behaves as nail, whether in powder or fragment form, while VN is similar to nail until 55% of relative humidity, then this model overstates the nail ability to absorb water. It is also noteworthy that sorption isotherm does not depend on sample form and thickness. Values obtained of moisture content for NC are slightly lower than values found in the literature, where the moisture content is about 10-15 % for a relative humidity of 45% (Baden et al., 1973; Egawa et al., 2003; Farran et al., 2008). These differences are due to the chosen temperature, fixed here at 30 °C. Moreover, nail plate absorption ability depends on individual morphologies (Egawa et al., 2005) and samples can lose water after clipping (Stern et al., 2007).

On the other hand, the room temperature dependence of the materials was investigated under fixed relative humidity conditions, *i.e.* 45%. The drying step consisted on an increase

from 5 to 55°C of temperature. The evolution of samples weight is shown in Supporting Information (**Fig. S5**) and results are summarized in **Table 3**. Besides the importance to consider powders instead of fragments for samples comparison, they show that NC and KF have the same temperature dependence. The difference is greater with VN whose temperature dependence is less important.

3.4. Nail lacquer adhesion on nail and models

The adhesion on nail and on models was investigated with three nails lacquers (NLs) (see experimental part).

Thermodynamic adhesion

According to the thermodynamic adhesion condition, adhesion to a substrate takes place if the surface tension of the adhesive is equal to or inferior to the surface energy of the substrate (Venkatraman and Gale, 1998). Here, the surface tension of nail lacquers (26.4 mN.m^{-1}) is lower than the surface energy of NC, KF and VN (28, 30 and 35mN.m^{-1} respectively, with Owens-Wendt values). Hence, the spreading of nail lacquers is only limited by kinetics, which will depend on the viscosity, as reported in the literature for some esters used as emollients (Douguet et al., 2017). This explains the need of nail lacquer brushes. The limiting factor will not be the surface energy. Besides, the work of adhesion of the nail varnishes on the three substrates is similar: $W_a = 27$ mN.m^{-1} for NC, 28 mN.m^{-1} for KF and 30 mN.m^{-1}for VN (based on Owens-Wendt values).

Mechanical adhesion

A probe tack test was developed using a rotational rheometer to strip the nail lacquers from NC, KF and VN. The NLs were uniformly applied on the substrates, which were glued to the inferior plate of rheometer. The superior part of rheometer was glued to the NL before measuring the vertical force necessary to strip the NL (see experimental part). The maximum

21

stresses were obtained by dividing the maximum forces by stripped surface of NL from substrates. A typical stress strain curve is presented in **Fig. S6**. The final results are shown in **Fig. 5**. Each measurement has been repeated three times and standard deviations are given in Supporting Information. Two kinds of fractures were observed: an adhesive one, at the NL-substrate interface, and a cohesive one at the glue-NL interface. However, only the first type must be considered as it characterizes the adhesion to the substrate. All the values obtained are in the same range as those reported by Sögütlü *et al.*(Sögütlü et al., 2016) i.e around 1 N/mm². Comparing the three nail lacquers, the order of adhesion was: NL-GA > NL-GA-colored > NL-PA. Hence, as expected, NL-PA was less adherent than NL-GA. Indeed, the epoxy tosylamide resin in NL-GA possesses amine and sulfoxide functions able to form hydrogen bonds easier than the carbonyl found in polyester resin in NL-PA (see **Fig. S8**). On the other hand, the addition of pigments reduces adherence. Indeed, it is known that addition of pigments decreases the film flexibility, and so increases its brittleness (Felton and McGinity, 1999). Mizoguchi *et al.* have shown that with high PVC (Pigment Volume Content), the adherence can be worst (Mizoguchi and Ueki, 1960). Indeed, the film adhesion is mainly due to the resin and not to the pigments. Hence, increasing the pigment proportion also means reducing the resin proportion and decreasing the adhesion of the formulation to the substrate.
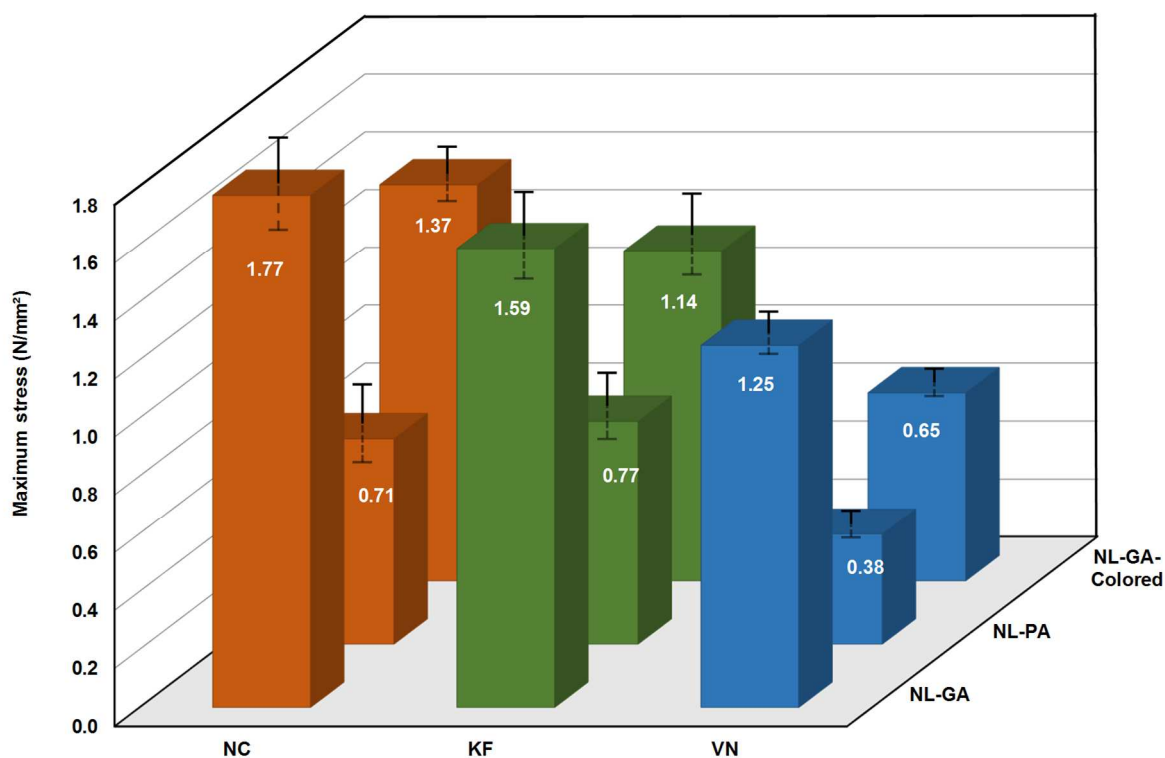
Fig. 5. Measured stress with adhesion test for nail, keratin film and Vitro-nail® respectively coated by nail lacquer known as having good adhesion (NL-GA), poor adhesion (NL-PA), and good adhesion charged with pigments (NL-GA-Colored). Standard deviations = 0.05 to 0.17 N/mm² (see SI for details).

Regarding the substrates, the highest values of maximum stress, and hence the better adherence, were obtained for NC with any nail lacquers. Maximum stress obtained with KF is a little lower, except for NL-PA. This lowest adherence could be due to a difference of roughness. Indeed, the NC surface allows a mechanical adhesion due to anchor points, whereas KF surface, twenty times softer, does not allow this type of adhesion. This weak difference shows that roughness is not a major factor for adhesion, though significant. For VN, adhesion is even weaker. As mentioned above, roughness plays a role when we compare VN to NC, but it is not sufficient to explain the gap of adhesion when we compare VN to KF. This difference is due to VN composition and its higher hydrophilicity and to its surface energy (high polar component). Indeed, VN has about twice more amide functions than NC and KF and although it forms hydrogen bonds with nail lacquers, it also absorbs a lot of water and functions in surface are no more available to interact with the nail lacquer components,

thus decreasing adhesion. Moreover, VN has not disulfide making it more permeable (Kerai et al., 2018), such as bovine hooves keratin (Kakkar et al., 2014). Accordingly, VN absorbs more water and as nail lacquer films are water sensitive (Murdan et al., 2015), the nail lacquer adhesion is weaker.

4.   Conclusion

In this study, keratin films and Vitro-nail®, two nail plate models based on biomaterials, were characterized and compared to nail clippings in terms of surface aspect, composition, surface energy and water absorption. Keratin films, due to its origin, are very similar to nail plates. The contact angles shaped by solvents, the surface energy, the composition and the water sorption are extremely close. Only the lipids amount, the roughness and the convex form of nail are different but the plate form of keratin film makes it easier to use for laboratory tests. Vitro-nails® are more hydrophilic and permeable due to probable higher proportions of amide functions and absence of disulfide bridges. Currently, only Vitro-nails®, which exhibit constant properties, are commercially available. Nevertheless, a commercialization of KF would be very useful as hair is available in huge amounts and usually free of charge. Furthermore, any difference or significant variability was detected in the properties of KF from different hair origin.

In parallel, an adhesion test was elaborated to measure the resistance to stripping of nail lacquers. The comparison of the adhesion of three different formulations correlated with the physicochemical characterization of the surfaces of the three materials allowed a better understanding of the adhesion mechanisms of nail lacquers on nail plate. Different adhesion theories were indeed verified comparing NC with KF and VN. The nail surface possesses a slight roughness permitting a significant mechanical adhesion, and a surface energy allowing a good wettability of nail lacquers. Chemical functions such as amides, amines, ammonium,

carboxylic acids/carboxylates and thiols are available for optimizing adhesion, in particular via hydrogen bonds and electrostatic interactions. Comparison with VN established the need of a substrate with a moderate hydrophilicity, which can be assessed by determining the polar component of the surface energy. Indeed, a too hydrophilic substrate decreases the adhesion of nail lacquers which are water sensitive. Therefore, for a better adhesion, the formulation of the nail lacquer should contain a polymer able to create hydrogen and ionic bonds. The nail lacquer must also have a surface tension inferior to 30 mN/m^{-1} and an optimized pigments content in order to prevent an increase of film brittleness and a too low resin proportion which would result in a lower adhesion.

References

Baden, H.P., 1970. The Physical Properties of Nail. J. Invest. Dermatol. 55, 115–122. https://doi.org/10.1111/1523-1747.ep12291628

Baden, H.P., Goldsmith, L.A., Fleming, B., 1973. A comparative study of the physicochemical properties of human keratinized tissues. Biochim. Biophys. Acta 322, 269–278. https://doi.org/10.1016/0005-2795(73)90303-6

Baden, H.P., Kvedar, J.C., 1993. Biology of nails, in: Dermatology in General Medicine. McGraw-Hill, New York, pp. 294–297.

Berg, J.C., 2010. The relationship of wetting and spreading behavior to adhesion, in: An Introduction to Intefarces & Colloids. World Scientific Publishing Co. Pte. Ltd., Singapore, pp. 258–277.

Chaudhury, M., Pocius, A., Dillard, D., 1997. Adhesion Science and Engineering. Hanser/Gardner, Cincinnati.

De Berker, D.A.R., André, J., Baran, R., 2007. Nail biology and nail science. Int. J. Cosmet. Sci. 29, 241–275. https://doi.org/10.1111/j.1467-2494.2007.00372.x

De Berker, D.A.R., Forslind, B., 2004. The structure and properties of nails and periungual tissues. Basic Clin. Dermatology 26, 409–464.

Doig, A.J., Baldwin, R.L., 1995. N and C capping preferences for all 20 amino acids in α helical peptides. Protein Sci. 4, 1325–1336. https://doi.org/10.1002/pro.5560040708

Douguet, M., Picarda, C., Savarya, G., Merlaudb, F., Loubat-bouleucb, N., Grisel, M., 2017. Spreading properties of cosmetic emollients: Use of synthetic skin surface to elucidate structural effect. colloids Surfaces B Biointerfaces 154, 307–314.

Egawa, M., Fukuhara, T., Takahashi, M., Ozaki, Y., 2003. Determining water content in human nails with a portable near-infrared spectrometer. Appl. Spectrosc. 57, 473–478. https://doi.org/10.1366/00037020360626032

Egawa, M., Ozaki, Y., Takahashi, M., 2005. In vivo measurement of water content of the fingernail and its seasonal change. Ski. Res. Technol. 12, 126–132. https://doi.org/10.1111/j.0909-752X.2006.00141.x

Farran, L., Ennos, A.R., Eichhorn, S.J., 2008. The effect of humidity on the fracture properties of human fingernails. J. Exp. Biol. 211, 3677–3681. https://doi.org/10.1242/jeb.023218

Felton, L.A., McGinity, J.W., 1999. Influence of pigment concentration and particle size on adhesion of an acrylic resin copolymer to tablet compacts. Drug Dev. Ind. Pharm. 25, 597–604. https://doi.org/10.1081/DDC-100102214

Gniadecka, M., Nielsen, O.F., Christensen, D.H., Wulf, H.C., 1998. Structure of water, proteins, and lipids in intact human skin, hair, and nail. J. Invest. Dermatol. 110, 393–398. https://doi.org/10.1046/j.1523-1747.1998.00146.x

Gómez, E.C., Anguiano Igea, S., Gómez Amoza, J.L., Otero Espinar, F.J., 2018. Evaluation of the promoting effect of soluble cyclodextrins in drug nail penetration. Eur. J. Pharm. Sci. 117, 270–278. https://doi.org/10.1016/j.ejps.2018.02.028

Gupchup, G. V., Zatz, J.L., 1999. Structural characteristics and permeability properties of the human nail: A review. J.Cosmet.Sci 50, 363–385.

Herries, D., 1985. Enzyme Structure and Mechanism (Second Edition), Biochemical Education. Freeman, Reading, Pennsylvania. https://doi.org/10.1016/0307-4412(85)90213-4

Kakkar, P., Madhan, B., Shanmugam, G., 2014. Extraction and characterization of keratin from bovine hoof: A potential material for biomedical applications. J. Korean Phys. Soc. 3, 1–9. https://doi.org/10.1186/2193-1801-3-596

Kendall, K., 2001. Molecular Adhesion and Its Application: The Sticky Universe. Kluwer/Plenum, New-York.

Kerai, L.V., Bardés, J., Hilton, S., Murdan, S., 2018. Two strategies to enhance ungual drug permeation from UV-cured films: Incomplete polymerisation to increase drug release and incorporation of chemical enhancers. Eur. J. Pharm. Sci. 123, 217–227. https://doi.org/10.1016/j.ejps.2018.07.049

Khengar, R.H., Jones, S.A., Turner, R.B., Forbes, B., Brown, M.B., 2007. Nail swelling as a pre-formulation screen for the selection and optimisation of ungual penetration enhancers. Pharm. Res. 24, 2207–2212. https://doi.org/10.1007/s11095-007-9368-3

Kinloch, A.J., 1987. Adhesion and Adhesives. Springer Science & Buisness Media.

Kobayashi, Y., Komatsu, T., Sumi, M., Numajiri, S., Miyamoto, M., Kobayashi, D., Sugibayashi, K., Morimoto, Y., 2004. In vitro permeation of several drugs through the human nail plate: Relationship between physicochemical properties and nail permeability of drugs. Eur. J. Pharm. Sci. 21, 471–477. https://doi.org/10.1016/j.ejps.2003.11.008

Kobayashi, Y., Miyamoto, M., Sugibayashi, K., Morimoto, Y., 1999. Drug permeation through the three layers of the human nail plate. J. Pharm. Pharmacol. 51, 271–278. https://doi.org/10.1211/0022357991772448

Lehtinen, J., 2013. Spectroscopic studies of human hair, nail, and saliva samples using a cantilever-based photoacoustic detection. Int. J. Thermophys. 34, 1559–1568. https://doi.org/10.1007/s10765-013-1488-x

Lusiana, Reichl, S., Müller-Goymann, C.C., 2013. Infected nail plate model made of human hair keratin for evaluating the efficacy of different topical antifungal formulations against Trichophyton rubrum in vitro. Eur. J. Pharm. Biopharm. 84, 599–605. https://doi.org/10.1016/j.ejpb.2013.01.015

Lusiana, Reichl, S., Müller-Goymann, C.C., 2011. Keratin film made of human hair as a nail plate model for studying drug permeation. Eur. J. Pharm. Biopharm. 78, 432–440. https://doi.org/10.1016/j.ejpb.2011.01.022

Lynch, M.H., O'Guin, W.M., Hardy, C., Mak, L., Sun, T.T., 1986. Acidic and basic hair/nail ("hard") keratins: Their colocalization in upper cortical and cuticle cells of the human hair follicle and their relationship to "Soft" keratins. J. Cell Biol. 103, 2593–2606. https://doi.org/10.1083/jcb.103.6.2593

Mertin, D., Lippold, B.C., 1997. In-vitro permeability of the human nail and of a keratin membrane from bovine hooves: Influence of the partition coefficient Octanol/Water and the water solubility of drugs on their permeability and maximum flux. J. Pharm. Pharmacol. 49, 30–34. https://doi.org/10.1111/j.2042-7158.1997.tb06747.x

Miron, D., Cornelio, R., Troleis, J., Mariath, J., Zimmer, A.R., Mayorga, P., Schapoval, E.E.S., 2014. Influence of penetration enhancers and molecular weight in antifungals permeation through bovine hoof membranes and prediction of efficacy in human nails. Eur. J. Pharm. Sci. 51, 20–25. https://doi.org/10.1016/j.ejps.2013.08.032

Mizoguchi, M., Ueki, K., 1960. Pigment Effects on the Adhesive Films Strength of Coating 1–6.

Monti, D., Saccomani, L., Chetoni, P., Burgalassi, S., Saettone, M.F., Mailland, F., 2005. In vitro transungual permeation of ciclopirox from a hydroxypropyl chitosan-based, water-soluble nail lacquer. Drug Dev. Ind. Pharm. 31, 11–17. https://doi.org/10.1081/DDC-43935

Murdan, S., 2002. Drug delivery to the nail following topical application. Int. J. Pharm. 236, 1–26. https://doi.org/10.1016/S0378-5173(01)00989-9

Murdan, S., Kerai, L., Hossin, B., 2015. To what extent do in vitro tests correctly predict the in vivo residence of nail lacquers on the nail plate? J. Drug Deliv. Sci. Technol. 25, 23–28. https://doi.org/10.1016/j.jddst.2014.11.002

Murdan, S., Milcovich, G., Goriparthi, G.S., 2011. An assessment of the human nail plate pH. Skin Pharmacol. Physiol. 24, 175–181. https://doi.org/10.1159/000324055

Murdan, S., Poojary, C., Patel, D.R., Fernandes, J., Haman, A., Saundh, P.S., Sheikh, Z., 2012. In vivo measurement of the surface energy of human fingernail plates. Int. J. Cosmet. Sci. 34, 257–262. https://doi.org/10.1111/j.1468-2494.2012.00711.x

Nogueiras-nieto, L., Gómez-amoza, J.L., Delgado-charro, M.B., Otero-espinar, F.J., 2011. Hydration and N-acetyl-l-cysteine alter the microstructure of human nail and bovine hoof : Implications for drug delivery. J. Control. Release 156, 337–344. https://doi.org/10.1016/j.jconrel.2011.08.021

Owens, D.K., Wendt, 1969. Estimation of the surface free energy of polymers. J. Appl. Polym. Sci. 13, 1741–1747. https://doi.org/10.1109/18.650986

Packham, D.E., 2011. Theories of fundamental adhesion, in: Handbook of Adhesion Technology. Springer, Berli Heildelberg, pp. 9–38.

Pittrof, F., Gerhards, J., Erni, W., Klecak, G., 1992. Loceryl® nail lacquer—realization of a new galenical approach to onychomycosis therapy. Clin. Exp. Dermatol. 17, 26–28. https://doi.org/10.1111/j.1365-2230.1992.tb00273.x

Rizi, K., Mohammed, I.K., Xu, K., Kinloch, A.J., Charalambides, M.N., Murdan, S., 2018. A systematic approach to the formulation of anti-onychomycotic nail patches. Eur. J. Pharm. Biopharm. 127, 355–365. https://doi.org/10.1016/j.ejpb.2018.02.032

Saeedi, P., Shavandi, A., Meredith-Jones, K., 2018. Nail Properties and Bone Health: A Review. J. Funct. Biomater. 9, 31. https://doi.org/10.3390/jfb9020031

Saner, M. V., Kulkarni, A.D., Pardeshi, C. V., 2014. Insights into drug delivery across the nail plate barrier. J. Drug Target. 22, 769–789. https://doi.org/10.3109/1061186X.2014.929138

Sharpe, L.H., 1998. Some Fundamental Issues in Adhesion: A Conceptual View. J. Adhes. 67, 277–289. https://doi.org/10.1080/00218469808011112

Söğütlü, C., Nzokou, P., Koc, I., Tutgun, R., Döngel, N., 2016. The effects of surface

roughness on varnish adhesion strength of wood materials. J. Coatings Technol. Res. 13, 863–870. https://doi.org/10.1007/s11998-016-9805-5

Sowa, M.G., Wang, J., Schultz, C.P., Ahmed, M.K., Mantsch, H.H., 1995. Infrared spectroscopic investigation of in vivo and ex vivo human nails. Vib. Spectrosc. 10, 49–56. https://doi.org/10.1016/0924-2031(95)00027-R

Stern, D.K., Diamantis, S., Smith, E., Wei, H., Gordon, M., Muigai, W., Moshier, E., Lebwohl, M., Spuls, P., 2007. Water content and other aspects of brittle versus normal fingernails. J. Am. Acad. Dermatol. 57, 31–36. https://doi.org/10.1016/j.jaad.2007.02.004

Täuber, A., Müller-Goymann, C.C., 2015. In vitro permeation and penetration of ciclopirox olamine from poloxamer 407-based formulations - Comparison of isolated human stratum corneum, bovine hoof plates and keratin films. Int. J. Pharm. 489, 73–82. https://doi.org/10.1016/j.ijpharm.2015.04.043

Venkatraman, S., Gale, R., 1998. Skin adhesives and skin adhesion. 1. Transdermal drug delivery systems. Biomaterials 19, 1119–1136. https://doi.org/10.1016/S0142-9612(98)00020-9

Walters, K.A., Abdalghafor, H.M., Lane, M.E., 2012. The human nail - Barrier characterisation and permeation enhancement. Int. J. Pharm. 435, 10–21. https://doi.org/10.1016/j.ijpharm.2012.04.024

Walters, K.A., Flynn, G.L., Marvel, J.R., 1983. Physicochemical characterization of the human nail: permeation pattern for water and the homologous alcohols and differences with respect to the stratum corneum. J. Pharm. Pharmacol. 35, 28–33. https://doi.org/10.1111/j.2042-7158.1983.tb04258.x

Wang, J.T; Sun, Y., 1999. Human nail and its topical treatment: Brief review of current research and development of topical antifungal drug delivery for onychomycosis

treatment. J.Cosmet.Sci 50, 71–76.

Wang, Y., Zhang, W., Yuan, J., Shen, J., 2016. Differences in cytocompatibility between collagen, gelatin and keratin. Mater. Sci. Eng. C 59, 30–34. https://doi.org/10.1016/j.msec.2015.09.093

Wessel, S., Gniadecka, M., Jemec, G.B.E., Wulf, H.C., 1999. Hydration of human nails investigated by NIR-FT-Raman spectroscopy. Biochim. Biophys. Acta 1433, 210–216. https://doi.org/10.1016/S0167-4838(99)00129-6

Williams, A.C., Edwards, H.G.M., Barry, B.W., 1994. Raman spectra of human keratotic biopolymers: Skin, callus, hair and nail. J. Raman Spectrosc. 25, 95–98. https://doi.org/10.1002/jrs.1250250113

Wu, S., 1982. Polymer Interface and Adhesion. Marcel Dekker, New-York.

Graphical Abstract